

## Structure and Bonding in $[\text{W}_{10}\text{O}_{32}]^{n-}$ Isopolyanions

Adam J. Bridgeman<sup>\*,†</sup> and Germán Cavigliasso<sup>‡,‡</sup>

Department of Chemistry, University of Hull, Kingston upon Hull HU6 7RX, U.K., and  
Department of Chemistry, University of Cambridge, Lensfield Road, Cambridge CB2 1EW, U.K.

Received: February 26, 2002; In Final Form: March 27, 2002

The structure and bonding in oxidized and reduced decatungstate anions have been investigated using density-functional methods. The computational–experimental agreement is good for the geometrical parameters of the oxidized species. The electronic structure of the anions has been probed with molecular-orbital, Mulliken–Mayer, and bonding-energy approaches, and the various analyses are in general accordance with spectroscopic evidence and theoretical models. The results have indicated that W–O interactions are largely W d–O p in character, and that  $\sigma$  and  $\pi$  bonds link the metal centers to terminal and bridging ( $\text{O}_{2c}$ ) oxygen atoms. Some W– $\text{O}_{2c}$  orbital interactions can be represented as  $[\text{W}_4\text{O}_4]$  or  $[\text{W}_6\text{O}_6]$  closed-loop structures, but these bonding modes have not been found to make a particularly outstanding contribution to the stability of the molecules. Mayer indexes correspond to (fractional) multiple, approximately single, and low-order character for terminal, bridging, and internal bonds, respectively, and the valency analysis has yielded similar bonding capacities for the different oxygen atoms. A distribution of the negative charge over all types of oxygen sites, and metal charges and orbital populations considerably different from the formal assignments have been obtained from the Mulliken analysis. Minor structural changes have been detected in reduced decatungstates, in accord with the general properties of the orbitals occupied by the added electrons.

### Introduction

Molybdenum and tungsten polyoxometalates constitute an immense class of compounds in number and diversity<sup>1,2</sup> and represent an extremely rich and active field of experimental research.<sup>2–4</sup> This research has covered the vast range of chemical and physical properties displayed by polyoxometalates, and the related applications, for example, to medicine, catalysis, solid-state technology, and chemical analysis. At the theoretical and computational levels, investigations of polyoxometalates have been comparatively more limited, but a number of calculations have been carried out using a variety of methods, including  $X\alpha$ ,<sup>5–9</sup> Hartree–Fock and density-functional techniques.<sup>10–20</sup>

Some properties of polyoxometalates are directly connected to the electronic structure of these clusters and can therefore be probed by computational approaches. Examples are the metal–oxygen closed loops that are observed in the typical polyanion structures and have been regarded as a type of macrocyclic bonding system constructed via multicentered  $\sigma$  and  $\pi$  interactions,<sup>21–26</sup> and the redox behavior that has been frequently rationalized in terms of molecular-orbital analyses of related monomeric complexes.<sup>1,2,26</sup>

We have recently studied,<sup>27–29</sup> using density-functional theory, several polyoxoanion systems, including the  $T_d$  and  $C_{2v}$  forms of  $[\text{W}_4\text{O}_{16}]^{8-}$  and the  $[\text{W}_6\text{O}_{19}]^{n-}$  and  $[\text{W}_7\text{O}_{24}]^{16-}$  clusters, and we have applied a number of analytical tools, such as molecular-orbital theory, population methods, and fragment-decomposition approaches, to explore, in particular, the nature and properties of closed loops, the molecular stability and reducibility and, in general, various structural and bonding

characteristics of these polyoxometalates. In the present work, we extend our computational investigations to the  $[\text{W}_{10}\text{O}_{32}]^{n-}$  anions.

The decatungstate anions have been the subject of rather extensive research, particularly in connection with the photocatalytic properties of these species.<sup>30</sup> In addition to the oxidized  $[\text{W}_{10}\text{O}_{32}]^{4-}$  form, the singly and doubly reduced  $[\text{W}_{10}\text{O}_{32}]^{5-}$  and  $[\text{W}_{10}\text{O}_{32}]^{6-}$  systems have been investigated and characterized experimentally,<sup>31,32</sup> and the observed (asymmetric) delocalization of the excess electrons has been analyzed using theoretical models.<sup>33,34</sup>

In this article, we report density-functional calculations on the oxidized and reduced forms of the decatungstate isopolyanions that complement the existing experimental and theoretical studies and provide further computational insight into the electronic structures of these clusters. We have carried out a structural characterization through full optimizations of the molecular geometries, and we present a detailed bonding analysis, including closed loops and redox behavior, based on molecular-orbital descriptions, Mulliken and Mayer methods, and molecular and fragment energetics.

### Computational Approach

All density-functional calculations reported in this work were performed with the ADF<sup>35,36</sup> or GAMESS-UK<sup>37</sup> programs. Functionals based on the Vosko–Wilk–Nusair (VWN)<sup>38</sup> form of the Local Density Approximation (LDA),<sup>39</sup> and on a combination (labeled BP86) of Becke’s 1988 exchange<sup>40</sup> and Perdew’s 1986 correlation<sup>41</sup> corrections to the LDA, and Slater-type-orbital (STO) basis sets of triple- $\zeta$  quality incorporating frozen cores and the ZORA relativistic approach (ADF O.1s and W.4f type IV)<sup>35,36</sup> were utilized in ADF calculations. The B3LYP<sup>42</sup> functional and Gaussian-type-orbital (GTO) basis sets of double- $\zeta$  quality and of the effective-core-potential type<sup>43–45</sup> were employed in GAMESS-UK calculations.

\* Corresponding author. Telephone: +44 1482 466549. Facsimile: +44 1482 466410. E-mail: A.J.Bridgeman@hull.ac.uk.

<sup>†</sup> University of Hull.

<sup>‡</sup> University of Cambridge.

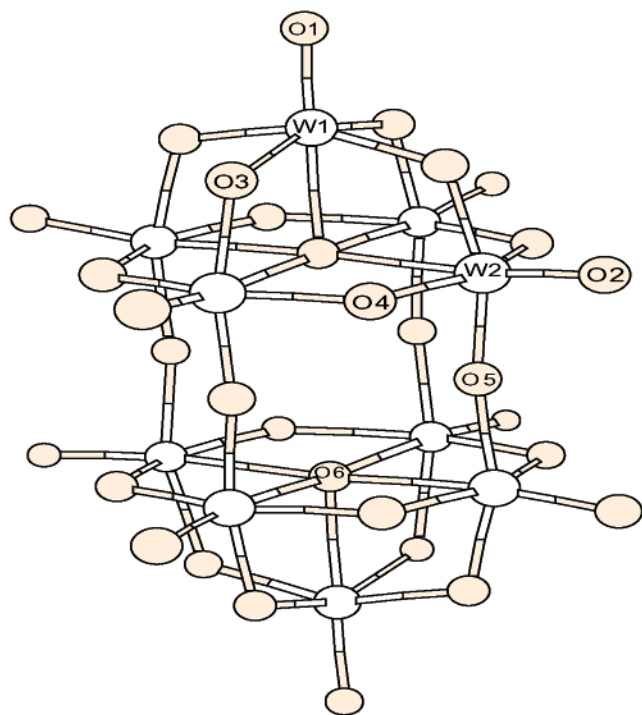


Figure 1. Structural and atom-labeling scheme for  $[\text{W}_{10}\text{O}_{32}]^{n-}$  anions.

TABLE 1: Optimized W–O Distances for the  $[\text{W}_{10}\text{O}_{32}]^{4-}$  Anion

parameter		calculation	experiment
W–O <sub>t</sub>	W1–O1	175	176
	W2–O2	174	170
W–O <sub>2c</sub>	W1–O3	193	190
	W2–O3	193	202
	W2–O4	193	191
	W2–O5	192	190
W–O <sub>5c</sub>	W1–O6	225	232
	W2–O6	233	230

The functional and basis-set choices were based on the results of tests performed on several  $[\text{MO}_4]$  and  $[\text{M}_2\text{O}_7]$  species.<sup>46,47</sup> Geometry optimizations were carried out using LDA methods, and data on thermochemistry and energetics were extracted from single-point BP86 or B3LYP calculations. Bond and valency indexes were obtained according to the definitions proposed by Mayer<sup>48,49</sup> and by Evarestov and Veryazov,<sup>50</sup> with a program<sup>51</sup> designed for their calculation from the ADF output file. Graphics of molecular orbitals were generated with the MOLEKEL<sup>52</sup> program.

## Results and Discussion

**Molecular Structure.** Structural and atom-labeling schemes for the  $[\text{W}_{10}\text{O}_{32}]^{n-}$  anions are presented in Figure 1. The optimized molecular geometry of the oxidized form is given in Table 1, which also includes experimental data taken from the compilations of Tytko and co-workers.<sup>53</sup> These results correspond to a  $D_{4h}$ -symmetry average of bond parameters in crystal structures.

The metal atoms in the decatungstate anions can be separated into “axial” (W1) and “equatorial” (W2) centers, and the oxygen atoms can be grouped in three different categories, terminal (O<sub>t</sub>: O1, O2), two-coordinate (O<sub>2c</sub>: O3, O4, O5), and five-coordinate (O<sub>5c</sub>: O6) sites. The calculated results are for an isolated molecule (solid-state effects have not been included), but the agreement with experimental data is reasonably good. The greatest deviations occur in the  $[\text{W1}-\text{O3}-\text{W2}]$  bridge

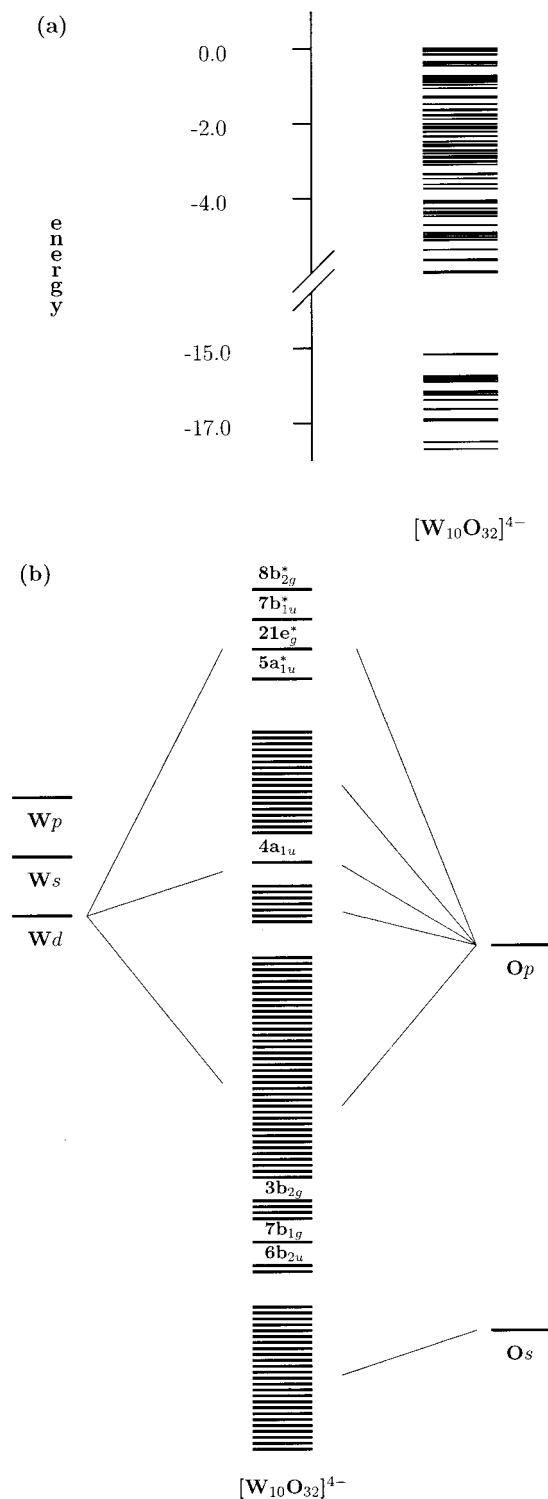
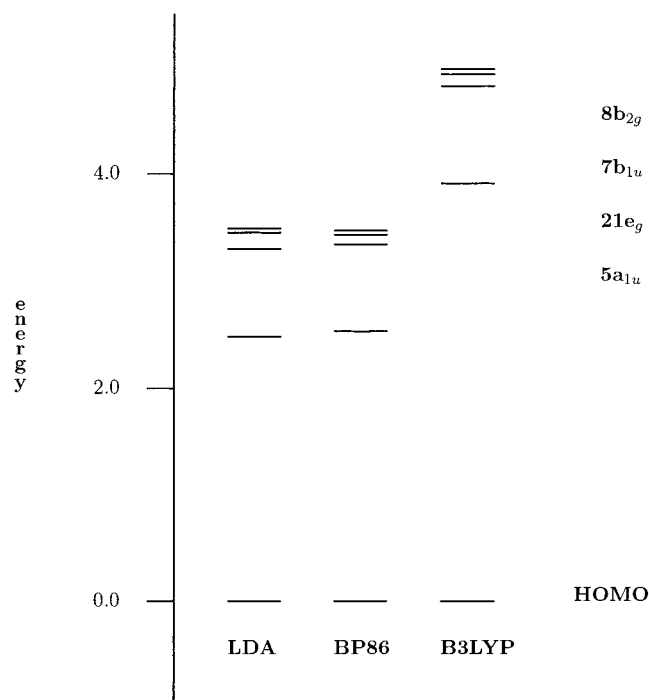


Figure 2. Eigenvalue (eV) diagram for occupied (valence) levels of  $[\text{W}_{10}\text{O}_{32}]^{4-}$  (a) and qualitative scheme showing predominant metal and oxygen contributions to the occupied and lowest virtual orbitals (b). In (a), the highest-occupied level (HOMO) is used as reference.

(which is predicted to be symmetric by the calculations but is found to be rather unsymmetric in the crystals) and in the (weak) W1–O6 bond.

**Electronic Structures. Molecular-Orbital Schemes.** An eigenvalue diagram for the occupied valence levels of the  $[\text{W}_{10}\text{O}_{32}]^{4-}$  anion and the predominant metal and oxygen contributions to the valence orbitals are shown in Figure 2. The scheme in part b is entirely qualitative in the sense that no



**Figure 3.** Eigenvalue (eV) diagram for the four lowest-unoccupied levels (LUMOs) of  $[\text{W}_{10}\text{O}_{32}]^{4-}$ . The highest-occupied level (HOMO) is used as reference.

**TABLE 2: Approximate Composition of Lowest Unoccupied Orbitals in the  $[\text{W}_{10}\text{O}_{32}]^{4-}$  Anion**

orbital	W1	W2	O	
5a <sub>1u</sub>	0.00	0.64	0.30	(O3)
21e <sub>g</sub>	0.00	0.65	0.29	(O3/O4)
7b <sub>1u</sub>	0.43	0.17	0.35	(O3/O4)
8b <sub>2g</sub>	0.52	0.12	0.33	(O3/O4)

accurate quantitative correlation exists among the positions of the atomic and molecular energy levels. It is intended to summarize the most general and representative characteristics of the electronic structure of the decatungstate anion by highlighting the major atomic contributions to the molecular orbitals.

The eigenvalue diagram in part a of Figure 2 shows two sets of energy levels, separated by a gap of approximately 10 eV. The levels in the low-lying set correspond to predominantly nonbonding combinations of O s orbitals. In the high-lying set, the majority of the lower-energy levels comprise a W–O bonding band of largely W d–O p character, whereas most of the higher-energy levels represent nonbonding combinations of O p orbitals. Some degree of overlap between the top of the W d–O p band and the bottom of the O p band is observed, and there is also a relatively high-lying (and “isolated”) W–O bonding level that has been identified in part b of Figure 2 by giving its (4a<sub>1u</sub>) symmetry label.

In addition to the W–O bonding band of occupied levels, the lowest virtual orbitals also represent W–O interactions but of antibonding character. These levels are particularly important in the reduced anions. The energetic ordering of the four lowest-unoccupied molecular orbitals (LUMOs) of  $[\text{W}_{10}\text{O}_{32}]^{4-}$ , obtained by the three computational methods utilized in this work, is shown in Figure 3, and their approximate compositions are given in Table 2. All calculations (at the LDA, BP86, and B3LYP levels of theory) predict that the first LUMO is the 5a<sub>1u</sub> orbital, which is plotted in Figure 4. It can be described as an extensively delocalized  $\pi$ -antibonding interaction involving the (“equatorial”) W2 and O3 atoms.

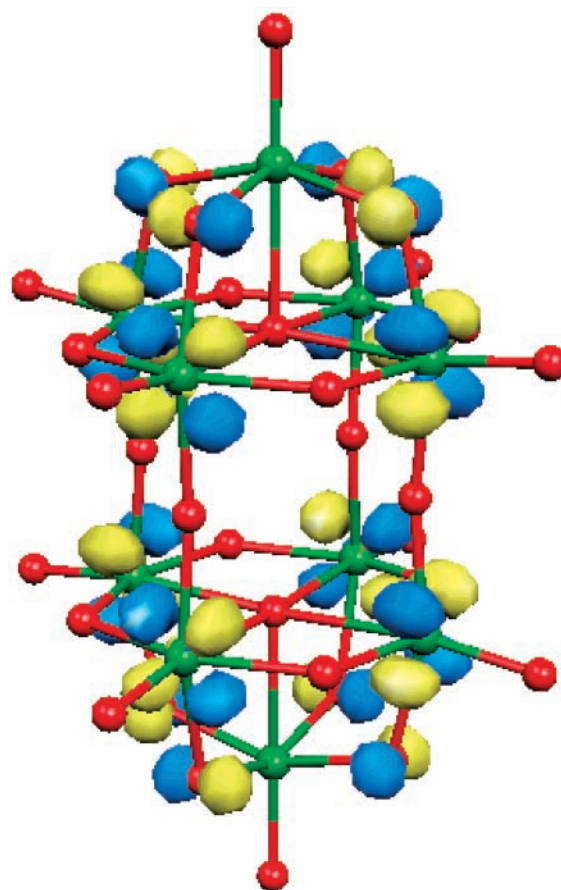


**Figure 4.** Spatial representation of the 5a<sub>1u</sub> orbital in the  $[\text{W}_{10}\text{O}_{32}]^{4-}$  anion.

*Closed Loops.* Nomiya and Miwa<sup>21</sup> have considered that delocalized  $\sigma$  and  $\pi$  bonding along the interpenetrating M–O closed loops observed in polyanions should behave as a structural-stability factor. This idea has been quantified in the form of an index ( $\eta$ ) defined as

$$\eta = \frac{\sum BC}{A} \quad (1)$$

where  $A$  is the number of octahedra constituting the polyanion cage,  $B$  is the number of  $\text{MO}_6$  units constituting the closed loop, and  $C$  is the number of closed loops (it should be noted that the polyanion cage is not necessarily identical with the whole structure, although it does comprise most of it<sup>21</sup>). It has also been suggested that structures with a higher  $\eta$  value should be more stable, but sometimes additional factors have been invoked in cases where this idea does not seem to work.<sup>21–25</sup>

For the  $[\text{W}_{10}\text{O}_{32}]^{n-}$  clusters, two types of closed loops have been proposed,<sup>21</sup> twelve-membered  $[\text{W}_6\text{O}_6]$  rings that are constructed by interconnecting  $[\text{W1}–\text{O3}–\text{W2}]$  and  $[\text{W2}–\text{O5}–\text{W2}]$  bridges along the “axial” direction and eight-membered  $[\text{W}_4\text{O}_4]$  rings involving the W2 and O4 atoms than lie in the “equatorial” planes. The molecular-orbital structures of these closed loops are shown in Figures 5 and 6. It is observed that both types of rings possess  $\sigma$  and  $\pi$  character, as suggested by Nomiya and Miwa. The  $\pi$ -like components of the bridging bonds involved in both types of rings can be described as in-plane and out-of-plane interactions, as in the  $[\text{W}_6\text{O}_{19}]^{2-}$  anion,<sup>28</sup> but only the latter are represented in Figures 5 and 6.

A measure of the relative contributions of the various metal–oxygen interactions to the molecular bonding energy ( $E_B$ ) of

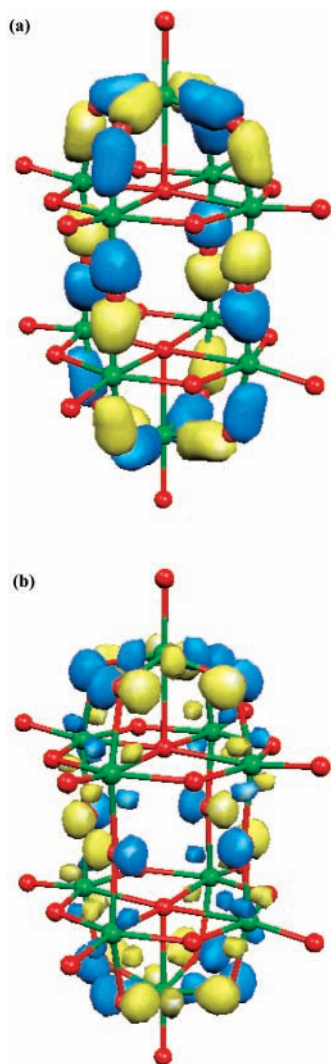
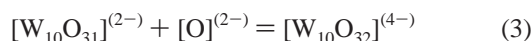


**Figure 5.** Spatial representation of (a)  $\sigma$  ( $6b_{2u}$  orbital) and (b)  $\pi$  ( $3b_{2g}$  orbital)  $[\text{W}_6\text{O}_6]$  closed loops.

the  $[\text{W}_{10}\text{O}_{32}]^{4-}$  polyanion can be obtained by combining

$$E_B = E_O + E_P + E_E \quad (2)$$

with the decomposition of the cluster as



In eq 2,  $E_O$ ,  $E_P$ , and  $E_E$  are, respectively, orbital-mixing, Pauli-repulsion, and electrostatic-interaction terms. Descriptions of the physical significance of these properties have been given by Landrum, Goldberg, and Hoffmann<sup>54</sup> and by Baerends and co-workers.<sup>36</sup> Both  $E_O$  and  $E_P$  represent orbital-interaction effects, but the former is stabilizing whereas the latter is destabilizing. The  $E_E$  contribution is primarily dominated by the nucleus–electron attractions and, therefore, has a stabilizing influence.

The total molecular bonding energy relative to the fragments is then given by

$$\Delta E_B = \Delta E_O + \Delta E_P + \Delta E_E \quad (4)$$

Results from application of eqs 3 and 4 are summarized in Table 3 and show that the  $\Delta E_B$  values for the  $\text{O}_t$  and  $\text{O}_{2c}$  atoms are all rather similar. In particular, the contributions from the terminal sites are slightly larger than those from the bridging

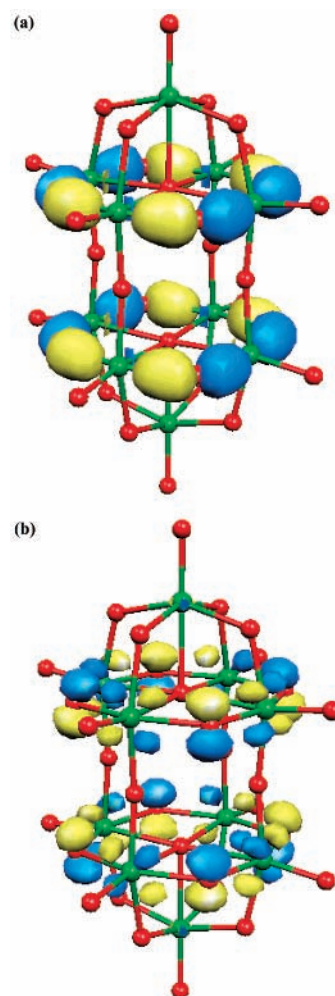


**Figure 6.** Spatial representation of (a)  $\sigma$  ( $7b_{1g}$  orbital) and (b)  $\pi$  ( $3b_{2g}$  orbital)  $[\text{W}_4\text{O}_4]$  closed loops.

**TABLE 3: Fragment Analysis ( $\Delta E_B$ , eV) for the  $[\text{W}_{10}\text{O}_{32}]^{4-}$  Anion (Results from BP86 Calculations)**

atom		$\Delta E_B$
$\text{O}_t$	$\text{O}_1$	−12.34
	$\text{O}_2$	−12.25
$\text{O}_{2c}$	$\text{O}_3$	−11.66
	$\text{O}_4$	−11.93
	$\text{O}_5$	−11.39
	$\text{O}_6$	−10.38
$\text{O}_{5c}$		

sites. Thus, these results do not suggest that the bonding modes involving W–O–W bridges should stand out as a stabilizing factor. It is also interesting to note that the bonding energy of  $\text{O}_{5c}$  atoms is of comparable magnitude to that of the other bridging ( $\text{O}_{2c}$ ) sites.

It should be noted that the choice of an oxide ion as a fragment in eq 3 is due, primarily, to computational convenience, as these calculations are required to be of the restricted type. This particular decomposition scheme is also convenient from a formal chemical standpoint.

**Reduced Anions.** The products of the one-electron and two-electron reductions of the decatungstate anion have been characterized by Chemseddine and co-workers<sup>31</sup> and by Duncan and Hill,<sup>32</sup> respectively. Both studies suggest that the general structure and  $D_{4h}$  symmetry of the oxidized cluster is retained in the reduced species. The low-temperature electron-spin-resonance (ESR) spectrum of  $[\text{W}_{10}\text{O}_{32}]^{5-}$ , and the  $^{183}\text{W}$  and  $^{17}\text{O}$  nuclear-magnetic-resonance (NMR) spectra of  $[\text{W}_{10}\text{O}_{32}]^{6-}$  have revealed an asymmetric distribution of the additional electrons,



**TABLE 4: Changes in Bond Distances ( $\delta(W-O)$ , pm) of Reduced Anions with Respect to  $[W_{10}O_{32}]^{4-}$** 

parameter		$[W_{10}O_{32}]^{5-}$	$[W_{10}O_{32}]^{6-}$
$\delta(W-O_e)$	$\delta(W1-O1)$	+0.8	+2.4
	$\delta(W2-O2)$	+0.8	+2.2
$\delta(W-O_{2c})$	$\delta(W1-O3)$	-0.5	-0.7
	$\delta(W2-O3)$	+3.2	+5.5
	$\delta(W2-O4)$	-0.7	-0.1
	$\delta(W2-O5)$	+0.4	+0.9
$\delta(W-O_{5c})$	$\delta(W1-O6)$	+3.8	+5.7
	$\delta(W2-O6)$	+0.5	+1.6

**TABLE 5: Symmetry Decomposition of the Orbital-Mixing ( $E_O$ ) Energy (eV) in the  $[W_{10}O_{32}]^{4-}$  Anion (Results from BP86 Calculations)**

term	energy
$a_{1g}$	-107.96
$a_{2g}$	-19.31
$b_{1g}$	-83.44
$b_{2g}$	-33.89
$e_g$	-216.09
$a_{1u}$	-14.01
$a_{2u}$	-112.29
$b_{1u}$	-28.93
$b_{2u}$	-87.19
$e_u$	-218.83
total	-921.93

which have been described as delocalized primarily over the “equatorial” tungsten sites.

Geometry optimizations for the  $[W_{10}O_{32}]^{5-}$  and  $[W_{10}O_{32}]^{6-}$  have been carried out using  $D_{4h}$  and  $C_s$  symmetry. The latter should allow for structural distortions and changes in the electron-density distribution (for example, localization) if these were favorable. The results obtained indicate that the overall structure of the oxidized system is largely retained, and that there is no appreciable difference in the nature and composition of the orbital occupied by the added electrons (Figure 4 and Table 2) in the  $D_{4h}$  and  $C_s$  forms. The latter have been found to be only slightly more stable than the former.

The changes in W–O bond distances of the reduced clusters with respect to the  $[W_{10}O_{32}]^{4-}$  anion are summarized in Table 4. The largest modifications are observed in the W2–O3 and W1–O6 bonds. The former are directly connected with the W2–O3 antibonding properties of the  $(5a_{1u})$  orbital accepting the added electrons. The effect on the W1–O6 distances is probably associated with increased electronic repulsions.

The relatively minor structural consequences brought about by reduction of the decatungstate anion may be explained in terms of a symmetry decomposition of the contributions to the orbital-mixing ( $E_O$ ) energy in eq 2. This is presented in Table 5. The  $a_{1u}$  component represents only a 0.015 fraction of the total orbital-mixing contribution to the bonding energy. Thus, although the  $5a_{1u}$  orbital is W–O antibonding, its effect on the bonding stability of the decatungstate system is comparatively small (the total  $E_O$  value diminishes by approximately 2–3% in each reduction step).

Duclosaud and Borshch<sup>33,34</sup> have carried out theoretical analyses of the electron distribution in the reduced systems. These authors have reported that the LUMO of  $[W_{10}O_{32}]^{4-}$ , obtained from extended Hückel calculations, is an orbital of  $a_{1g}$  symmetry. This is not supported by the present DF investigation. However, the general conclusions concerning the electron distribution in  $[W_{10}O_{32}]^{6-}$  are in agreement with the results of this work. The description of the doubly reduced decatungstate presented by Borshch<sup>34</sup> indicates that there is “negligibly small probability density at the terminal sites” and

**TABLE 6: Bonding Energetics (eV) of  $(5a_{1u})^n$  and  $(7b_{1u})^n$  ( $n: 1, 2$ ) Configurations of Reduced Anions (Results Given as  $\Delta E(5a_{1u} - 7b_{1u})$ ; from BP86 Calculations)**

energy term	$[W_{10}O_{32}]^{5-}$	$[W_{10}O_{32}]^{6-}$
$\Delta E_B$	-0.98	-2.07
$\Delta E_O$	-3.56	-5.43
$\Delta E_P$	+4.18	+5.38
$\Delta E_E$	-1.60	-2.02

that “the delocalized electron distribution is due not to strong electronic interaction through quasilinear oxygen bridges between equatorial layers but to the correlated delocalization of two electrons within two equatorial planes”.

These conclusions and the experimental spectroscopic evidence for the reduced decatungstate anions are consistent with the composition of the LUMO of  $[W_{10}O_{32}]^{4-}$  yielded by the present density-functional calculations. The electron density associated with this orbital is largely distributed over the “equatorial” planes defined by the W2–O3 bonds, with negligible contributions from the “axial” W1 sites and the O5 atoms. In addition, the calculations predict that the  $[W_{10}O_{32}]^{6-}$  anion should be diamagnetic, in accordance with experimental evidence.<sup>31,32</sup>

Borshch<sup>34</sup> has also described the excess-electron delocalization over “equatorial” sites as surprising in principle as the concentration of density at the more distant axial centers appears more favorable if electron-repulsion effects are considered. This argument can be analyzed in more detail using eq 2. Table 2 shows that the first unoccupied orbital with significant W1 character occurs as the  $7b_{1u}$  level. Calculations have been carried out for the  $(7b_{1u})^1$  and  $(7b_{1u})^2$  configurations of  $[W_{10}O_{32}]^{5-}$  and  $[W_{10}O_{32}]^{6-}$ , respectively, and the results obtained are compared in Table 6 with those for the  $(5a_{1u})^1$  and  $(5a_{1u})^2$  configurations.

The  $(5a_{1u})^n$  systems are more stable than the  $(7b_{1u})^n$  systems, as expected from the respective positions of the  $5a_{1u}$  and  $7b_{1u}$  molecular orbitals in Figure 3. The W2-based states are strongly favored by orbital-mixing effects and to some extent by electrostatic factors, whereas those involving W1 atoms exhibit a significantly reduced Pauli repulsion. Thus, these results support the argument suggested by Borshch, that is, the gain in energy due to delocalization over the W2 sites surpasses the loss associated with repulsive effects and becomes a decisive stability factor.

**Population Methods.** The results presented in this section are based on Mulliken and Mayer methodology. These methods are known to exhibit basis-set dependence, but (relative) Mulliken charges and Mayer bond indexes can nonetheless provide valuable chemical information for inorganic systems, if uniformity and consistency of the basis sets are maintained.<sup>55</sup> Furthermore, Mulliken analysis has been described as “not an arbitrary choice ... but consistent with the internal structure of the molecular-orbital formalism”.<sup>48</sup>

**Mulliken Analysis.** Mulliken charges for all atoms and metal basis-function populations are given in Tables 7 and 8, respectively. The results correspond to metal  $d^3-d^4$  electronic configurations, in contrast to the formal  $d^0$  assignment, and the charges are considerably smaller than the formal oxidation states. Although some increase in d-orbital populations (and consequently lower charges) is observed in  $[W_{10}O_{32}]^{5-}$  and  $[W_{10}O_{32}]^{6-}$ , the effects of reduction are relatively small. The s and p orbitals are sparingly populated, in accordance with the molecular-orbital analysis indicating predominant participation of W d functions in W–O bonds, and are largely unaffected by reduction.

The oxygen values reveal that the negative charge is distributed over all types of atoms, and that the terminal sites

**TABLE 7: Mulliken Charges for Metal and Oxygen Atoms in Oxidized and Reduced Anions**

atom		$[\text{W}_{10}\text{O}_{32}]^{4-}$	$[\text{W}_{10}\text{O}_{32}]^{5-}$	$[\text{W}_{10}\text{O}_{32}]^{6-}$
W	W1	+2.27	+2.23	+2.19
	W2	+2.35	+2.30	+2.24
$\text{O}_t$	O1	-0.77	-0.82	-0.85
	O2	-0.74	-0.77	-0.81
$\text{O}_{2c}$	O3	-0.88	-0.89	-0.90
	O4	-0.89	-0.90	-0.90
	O5	-0.87	-0.88	-0.87
$\text{O}_{5c}$	O6	-1.12	-1.11	-1.11

**TABLE 8: Populations of Metal Basis Functions in Oxidized and Reduced Anions**

molecule	W1			W2		
	s	p	d	s	p	d
$[\text{W}_{10}\text{O}_{32}]^{4-}$	0.10	0.15	3.47	0.10	0.14	3.40
$[\text{W}_{10}\text{O}_{32}]^{5-}$	0.12	0.15	3.50	0.11	0.14	3.45
$[\text{W}_{10}\text{O}_{32}]^{6-}$	0.13	0.14	3.54	0.12	0.14	3.49

**TABLE 9: Mayer Indexes for Oxidized and Reduced Anions (Results from Classical Bond-valence Analysis Given in Parentheses)**

parameter		$[\text{W}_{10}\text{O}_{32}]^{4-}$	$[\text{W}_{10}\text{O}_{32}]^{5-}$	$[\text{W}_{10}\text{O}_{32}]^{6-}$
W– $\text{O}_t$	W1–O1	1.65 (1.50)	1.60	1.56
	W2–O2	1.69 (1.53)	1.66	1.63
W– $\text{O}_{2c}$	W1–O3	0.78 (0.97)	0.81	0.84
	W2–O3	0.72 (0.97)	0.67	0.64
	W2–O4	0.76 (0.97)	0.76	0.76
	W2–O5	0.76 (0.99)	0.77	0.78
W– $\text{O}_{5c}$	W1–O6	0.27 (0.44)	0.26	0.26
	W2–O6	0.23 (0.37)	0.24	0.24

in the reduced species accept, individually, considerably more excess charge than the bridging sites. These observations are qualitatively similar to those made by Tytko and co-workers from results based on a bond-valence model for polyoxometalates.<sup>53,56</sup>

**Bond-Order Analysis.** Mayer bond-order indexes are given in Table 9. For the oxidized anion, additional results have been obtained with a bond-valence model based on the following relationship<sup>53</sup>

$$\log s = \frac{(d_0 - d)}{B} \quad (5)$$

where  $s$  is the bond valence,  $d_0$  is the single-bond length,  $B$  defines the slope of the bond length-bond valence functions, and  $d$  is a calculated bond distance. The agreement between computational and classical predictions is satisfactory for all types of bonds.

For all anions, the Mayer indexes reflect the trends in the W–O distances and reveal weak W– $\text{O}_{5c}$  bonds, approximately single character for W– $\text{O}_{2c}$  bonds, and significant but, as previously observed,<sup>53</sup> not maximized W– $\text{O}_t$  multiple bonding. The changes in the bond orders for the reduced species, with respect to  $[\text{W}_{10}\text{O}_{32}]^{4-}$ , are in general accord with the structural, orbital, and charge effects.

The Mayer indexes for terminal bonds decrease on reduction primarily as a consequence of the higher ionic character associated with the increased  $\text{O}_t$  charges. For the  $\text{O}_{2c}$  (O4, O5) atoms not involved in accepting the added electrons, the geometrical and charge-related modifications are small, and the Mayer-index values indicate that the bonding is not unfavorably affected. A similar observation applies to the W– $\text{O}_{5c}$  interactions, even though the W1–O6 bonds lengthen considerably. The O3 atoms participate in the composition of the LUMO of

**TABLE 10: Covalency and Full-Valency Indexes for Oxygen Atoms in the  $[\text{W}_{10}\text{O}_{32}]^{4-}$  Anion**

atom		covalency	full valency
$\text{O}_t$	O1	2.00	2.27
	O2	2.04	2.28
$\text{O}_{2c}$	O3	1.84	2.20
	O4	1.86	2.22
	O5	1.88	2.22
$\text{O}_{5c}$	O6	1.44	2.04

the oxidized cluster, and the decreasing W2–O3 bond orders reflect the effect of the antibonding character of these W–O interactions. The second (W1–O3) bond to the O3 sites is, however, not directly influenced by the occupation of the  $5a_{1u}$  orbital, and the structural and Mayer results suggest that it may become slightly stronger in the reduced anions.

The relatively small decrease in the value of the W2–O3 index, and in general the minor structural and bonding changes caused by reduction, are consistent with the fact that the additional electrons occupy an orbital that is not strongly antibonding and makes a comparatively minor contribution to the stability of the polyanions (Table 5). These results differ significantly from the redox behavior of monomeric  $[\text{WOC}_5]^{n-}$  complexes<sup>57</sup> that are frequently used as simple models for the polymeric species and supports the idea (proposed by Nomiya and Miwa<sup>21</sup>) that the whole polyanion cage, and not only the properties of the individual  $\text{MO}_6$  octahedra, should play an important role in electron-transfer phenomena.

**Oxygen Valency.** Covalency and full-valency indexes for the oxygen atoms are shown in Table 10. The former are calculated as a sum of all Mayer indexes for a particular atom (and therefore include some contributions, for example, O–O interactions, that may be small but not necessarily negligible), whereas the latter are a combined measure of covalent (covalency) and ionic (electrovalency) bonding based on Mayer and Mulliken results.

The weakness of internal bonds in polyanions has been frequently ascribed to the trans influence of the strong M– $\text{O}_t$  interactions.<sup>1,2</sup> This effect is evident in the values of distances and orders for individual W– $\text{O}_{5c}$  bonds in the  $[\text{W}_{10}\text{O}_{32}]^{n-}$  anions. However, the differences in the covalency values are much smaller than those observed for the individual bond orders, and the full-valency indexes for the various types of oxygen atoms are all rather similar (as are the  $\Delta E_B$  contributions in the fragment analysis of Table 3) despite the variety of W–O interactions and coordination environments.

These results are thus supportive of the observations made by Tytko and co-workers,<sup>53</sup> who have pointed out that, although the individual trans-to-oxo M–O bonds are longest and weakest, the O atoms involved interact with a higher number of metal centers and may be as (or even more) strongly bound overall as the terminal (oxo) ligands are.

## Conclusion

The molecular and electronic structures of  $[\text{W}_{10}\text{O}_{32}]^{n-}$  isopolyanions have been investigated using density-functional methods. The computational results for the geometrical parameters of the oxidized cluster compare well with experimental data from crystal structures, and the general bonding description of oxidized and reduced species is in satisfactory agreement with spectroscopic information and theoretical models.

The molecular-orbital and population analyses have indicated that the W–O interactions are largely of W d–O p character and can be characterized as (fractional) multiple terminal bonds, approximately single bridging ( $\text{O}_{2c}$ ) bonds, and low-order

internal ( $O_{5c}$ ) bonds, in accord with structural and bond-valence data. Bonds of  $\sigma$  and  $\pi$  nature are formed between the metal centers and the terminal and bridging oxygen atoms, and some  $W-O_{2c}$  orbital interactions can be described in terms of the  $[W_4O_4]$  and  $[W_6O_6]$  closed loops proposed by Nomiya and Miwa. The valency and bonding-energy results have revealed similarities in the overall bonding capacity and strength of the various oxygen sites, and the latter have not indicated that there is a special stabilizing contribution associated with the  $[W-O_{2c}]$  bridges.

Minor structural changes have been detected in the singly and doubly reduced anions. This result is consistent with the general properties of the orbitals occupied by the added electrons, which have been found not to strongly affect the stability of the polyanions, being only slightly antibonding. The present calculations indicate that these orbitals are extensively delocalized over "equatorial" (but not "axial") sites, as suggested by previous spectroscopic measurements and theoretical modeling.

The Mulliken analysis has yielded a distribution of the negative charge over all types of oxygen sites and has suggested that the excess charge in reduced anions appears to be more readily accepted by  $O_t$  than  $O_b$  atoms. The metal charges and orbital populations have been found to be considerably different from the formal oxidation states and electronic configurations.

**Acknowledgment.** We thank EPSRC, the Cambridge Overseas Trust, Selwyn College (Cambridge), and the University of Hull for financial support, and the Computational Chemistry Working Party for access to computational facilities in the Rutherford Appleton Laboratory.

## References and Notes

- (1) Pope, M. T. *Heteropoly and Isopoly Oxometalates*; Springer-Verlag: Heidelberg, 1983.
- (2) Pope, M. T.; Müller, A. *Ang. Chem., Int. Ed. Eng.* **1991**, *30*, 34.
- (3) Baker, L. C. W.; Glick, D. C. *Chem. Rev.* **1998**, *98*, 3.
- (4) Pope, M. T.; Müller, A., Eds. *Polyoxometalates: from Platonic Solids to Anti-retroviral Activity*; Kluwer: Dordrecht, The Netherlands 1994.
- (5) Eguchi, K.; Seiyama, T.; Yamazoe, N.; Katsuki, S.; Taketa, H. *J. Catal.* **1988**, *111*, 336.
- (6) Taketa, H.; Katsuki, S.; Eguchi, K.; Seiyama, T.; Yamazoe, N. *J. Phys. Chem.* **1986**, *90*, 2959.
- (7) Xiao, S. X.; Ji, J.; Chen, T. L.; Cai, T. X.; Yan, G. S. *THEOCHEM* **1990**, *63*, 33.
- (8) Chen, T. L.; Ji, J.; Xiao, S. X.; Cai, T. X.; Yan, G. S. *Int. J. Quantum Chem.* **1992**, *44*, 1015.
- (9) Cai, T.; Chen, Z. D.; Wang, X. Z.; Li, L. M.; Lu, J. X. *Prog. Nat. Sci.* **1997**, *7*, 554.
- (10) Rohmer, M.-M.; Ernenwein, R.; Ulmschneider, M.; Wiest, R.; Bénard, M. *Int. J. Quantum Chem.* **1991**, *40*, 723.
- (11) Kempf, J.-Y.; Rohmer, M.-M.; Poblet, J.-M.; Bo, C.; Bénard, M. *J. Am. Chem. Soc.* **1992**, *114*, 1136.
- (12) Rohmer, M.-M.; Bénard, M. *J. Am. Chem. Soc.* **1994**, *116*, 6959.
- (13) Devémy, J.; Rohmer, M.-M.; Bénard, M.; Ernenwein, R. *Int. J. Quantum Chem.* **1996**, *58*, 267.
- (14) Rohmer, M.-M.; Devémy, J.; Wiest, R.; Bénard, M. *J. Am. Chem. Soc.* **1996**, *118*, 13007.
- (15) Maestre, J. M.; Sarasa, J. P.; Bo, C.; Poblet, J. M. *Inorg. Chem.* **1998**, *37*, 3071.
- (16) Maestre, J. M.; Poblet, J. M.; Bo, C.; Casañ-Pastor, N.; Gomez-Romero, P. *Inorg. Chem.* **1998**, *37*, 3444.
- (17) Dolbecq, A.; Guirauden, A.; Fourmigué, M.; Boubekur, K.; Batail, P.; Rohmer, M.-M.; Bénard, M.; Coulon, C.; Sallé, M.; Blanchard, P. *J. Chem. Soc., Dalton Trans.* **1999**, 1241.
- (18) Maestre, J. M.; López, X.; Bo, C.; Poblet, J. M.; Casañ-Pastor, N. *J. Am. Chem. Soc.* **2001**, *123*, 3749.
- (19) López, X.; Maestre, J. M.; Bo, C.; Poblet, J. M. *J. Am. Chem. Soc.* **2001**, *123*, 9571.
- (20) Rohmer, M.-M.; Bénard, M.; Blaudeau, J.-P.; Maestre, J.-M.; Poblet, J.-M. *Coord. Chem. Rev.* **1998**, *178-180*, 1019.
- (21) Nomiya, K.; Miwa, M. *Polyhedron* **1984**, *3*, 341.
- (22) Nomiya, K.; Miwa, M. *Polyhedron* **1985**, *4*, 89.
- (23) Nomiya, K.; Miwa, M. *Polyhedron* **1985**, *4*, 675.
- (24) Nomiya, K.; Miwa, M. *Polyhedron* **1985**, *4*, 1407.
- (25) Nomiya, K. *Polyhedron* **1987**, *6*, 309.
- (26) King, R. B. *Inorg. Chem.* **1991**, *30*, 4437.
- (27) Bridgeman, A. J.; Cavigliasso, G. *Polyhedron* **2001**, *20*, 3101.
- (28) Bridgeman, A. J.; Cavigliasso, G. *Inorg. Chem.* **2002**, *41*, 1761.
- (29) Bridgeman, A. J.; Cavigliasso, G. *J. Chem. Soc., Dalton Trans.* **2002**, 2244.
- (30) Tanielian, C. *Coord. Chem. Rev.* **1998**, *180*, 1165.
- (31) Chemseddine, A.; Sanchez, C.; Livage, J.; Launay, J. P.; Fournier, M. *Inorg. Chem.* **1984**, *23*, 2609.
- (32) Duncan, D. C.; Hill, C. L. *Inorg. Chem.* **1996**, *35*, 5828.
- (33) Duclusaud, H.; Borshch, S. A. *Chem. Phys. Lett.* **1998**, *290*, 526.
- (34) Borshch, S. A. *Inorg. Chem.* **1998**, *38*, 3116.
- (35) ADF2000.02. Baerends, E. J.; Ellis, D. E.; Ros, P. *Chem. Phys.* **1973**, *2*, 41. Versluis, L.; Ziegler, T. *J. Chem. Phys.* **1988**, *322*, 88. te Velde, G.; Baerends, E. J. *J. Comput. Phys.* **1992**, *99*, 84. Fonseca Guerra, G.; Snijders, J. G.; te Velde, G.; Baerends, E. J. *Theor. Chem. Acc.* **1998**, *99*, 391.
- (36) te Velde, G.; Bickelhaupt, F. M.; Baerends, E. J.; FonsecaGuerra, C.; van Gisbergen, S. J. A.; Snijders, J. G.; Ziegler, T. *J. Comput. Chem.* **2001**, *22*, 931.
- (37) GAMESS-UK. A package of ab initio programs written by M. F. Guest, J. H. van Lenthe, J. Kendrick, K. Schoffel and P. Sherwood, with contributions from R. D. Amos, R. J. Buenker, M. Dupuis, N. C. Handy, I. H. Hillier, P. J. Knowles, V. Bonacic-Koutecky, W. von Niessen, R. J. Harrison, A. P. Rendell, V. R. Saunders, and A. J. Stone.
- (38) Vosko, S. H.; Wilk, L.; Nusair, M. *Can. J. Phys.* **1980**, *58*, 1200.
- (39) Kohn, W.; Sham, L. J. *Phys. Rev.* **1965**, *140*, A1133.
- (40) Becke, A. D. *Phys. Rev. A* **1988**, *38*, 3098.
- (41) Perdew, J. P. *Phys. Rev. B* **1986**, *33*, 8822.
- (42) Stephens, P. J.; Devlin, F. J.; Chabalowski, C. F.; Frisch, M. J. *J. Phys. Chem.* **1994**, *98*, 11623.
- (43) Stevens, W. J.; Basch, H.; Krauss, M. *J. Chem. Phys.* **1984**, *81*, 6026.
- (44) Stevens, W. J.; Jasien, P. G.; Krauss, M.; Basch, H. *Can. J. Chem.* **1992**, *70*, 612.
- (45) Cundari, T. R.; Stevens, W. J. *J. Chem. Phys.* **1993**, *98*, 5555.
- (46) Bridgeman, A. J.; Cavigliasso, G. *Polyhedron* **2001**, *20*, 2269.
- (47) Bridgeman, A. J.; Cavigliasso, G. *J. Phys. Chem. A* **2001**, *105*, 7111.
- (48) Mayer, I. *Chem. Phys. Lett.* **1983**, *97*, 270.
- (49) Mayer, I. *Int. J. Quantum Chem.* **1984**, *26*, 151.
- (50) Evarestov, R. A.; Veryazov, V. A. *Theor. Chim. Acta* **1991**, *81*, 95.
- (51) MAYER. A program to calculate Mayer bond-order indexes from the output of the electronic structure packages GAMESS-UK, GAUSSIAN, and ADF, written by A. J. Bridgeman, University of Hull 2001. Available from the author on request.
- (52) MOLEKEL: An Interactive Molecular Graphics Tool; Portmann S.; Lüthi, H. P. *Chimia* **2000**, *54*, 766.
- (53) Tytko, K. H.; Mehmkke, J.; Fischer, S. *Struct. Bonding* **1999**, *93*, 129.
- (54) Landrum, G. A.; Goldberg, N.; Hoffmann, R. *J. Chem. Soc., Dalton Trans.* **1997**, 3605.
- (55) Bridgeman, A. J.; Cavigliasso, G.; Ireland, L. R.; Rothery, J. *J. Chem. Soc., Dalton Trans.* **2001**, 2095.
- (56) Tytko, K. H. *Struct. Bonding* **1999**, *93*, 67.
- (57) Bridgeman, A. J.; Cavigliasso, G. *J. Chem. Soc., Dalton Trans.* **2001**, 3556.